Information, Error, and Imaging in Deadtime-Perturbed Doubly Stochastic Poisson Counting Systems

MALVIN CARL TEICH, SENIOR MEMBER, IEEE, AND BARRY I. CANTOR

Abstract—The detection of a fluctuating signal in the presence of noise is considered for a doubly stochastic Poisson counting system that is subject to fixed nonparalyzable detector deadtime. Explicit expressions are obtained for the likelihood-ratio detection of a modulated source of arbitrary statistics in the presence of Poisson noise counts. Receiver operating characteristics (ROC curves) are presented for an unmodulated (amplitude-stabilized) source with detector deadtime as a parameter; increasing deadtime causes a decrease in the probability of detection for a fixed false-alarm rate. Probability of error curves are presented for an amplitude-stabilized source, both in the absence of modulation and in the presence of triangular modulation, illustrating the deleterious effects of modulation, noise, and deadtime on receiver performance. Expressions for the average mutual information and channel capacity of the system are obtained and graphically presented for the simple counting receiver and for the maximum-likelihood counting receiver; the channel capacity decreases with decreasing signal level and with increasing deadtime and modulation depth. Representative examples of the appropriate counting distributions are provided. Finally, a maximum-likelihood estimate of the mean signal level is obtained for a simple image detection system with a deadtime-perturbed counting array. An expression for the statistical confidence level of the estimate is also obtained. The results are valid for an arbitrary deadtime-perturbed doubly stochastic Poisson counting system and as such are expected to find application in a broad variety of disciplines including photon counting and lightwave communications, operations research, nuclear particle counting, and neural counting and psychophysics.

I. Introduction

In the past decade there has been considerable effort devoted to the analysis of systems that convert a continuous source variable into a discrete counting process. Perhaps the earliest study of this kind was carried out in 1920 by Greenwood and Yule [1], who in the course of studying the industrial accident rate in a British munitions factory, considered the Poisson transform of a probability density function specifying individual proneness to accident. Though much of the subsequent work on these compound or doubly stochastic Poisson processes, as they are now called, has specifically dealt with the photon-counting detection of light in a fixed time interval, first considered by Purcell [2] and Mandel [3], the formalism has also been applied to neural counting and psychophysics by McGill [4]. Teich and McGill [5] recently demonstrated that McGill's auditory neural counting model and Mandel's semiclassical photon-counting description [3] are in fact identical from a mathematical point of view and can be formally represented in terms of Greenwood and Yule's compound Poisson distribution. This equivalence was explicitly demonstrated for McGill's noncentral negative binomial distribution and Peřina's [6], [7] multimode confluent hypergeometric distribution for a coherent signal imbedded in chaotic noise (an excellent approximation for the radiation from an amplitude-stabilized single-mode laser operated well above the threshold of oscillation). For all of these problems, the underlying Poisson behavior can arise from the occurrence of independent events [8] or from the superposition of a large number of arbitrary stochastic point processes [9]-[11].

For an optical system, forward photon-counting distributions have been studied from both a quantum-mechanical [7], [12]-[14] and a semiclassical [3], [7] point of view for a broad range of incident field statistics [7] and modulation formats [15]-[20]. (Recently, increasing consideration has been given to the doubly stochastic Poisson process where attention is directed to the more general photoelectron arrival times [21] rather than to their number in a fixed time interval as considered here.) Calculations for direct-detection likelihood-ratio receiver performance [22]-[31] and information rate [32]-[36] have also been carried out by a number of researchers.

One factor that can substantially impair the performance of this kind of counting system—particularly at high data rates—is deadtime. Fortunately, the nonparalyzable deadtime-perturbed problem can be treated rather easily from a mathematical point of view since Cantor and Teich [37] have obtained a closed-form expression for the deadtime-modified counting distribution for a doubly stochastic Poisson counting

Manuscript received June 6, 1978. This work was supported in part by the Joint Services Electronics Program (U.S. Army, U.S. Navy, and U.S. Air Force) under Contract DAAG29-77-C-0019, and in part by the National Science Foundation.

M. C. Teich is with the Department of Electrical Engineering and Computer Science, Columbia Radiation Laboratory, Columbia University, New York, NY 10027.

B. I. Cantor was with the Department of Electrical Engineering and Computer Science, Columbia University, New York, NY 10027. He is now with the Babcock and Wilcox Company, Lynchburg Research Center, Lynchburg, VA 24505.

0018-9197/78/1200-0993$00.75

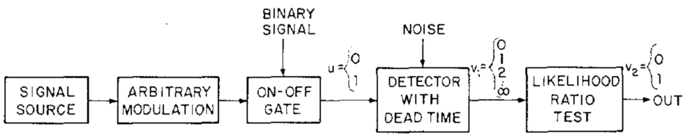

Fig. 1. Block diagram of the binary-gated deadtime-modified likelihood-ratio counting receiver for detecting a fluctuating signal.

process. The special case of the deadtime-modified simple Poisson distribution had been previously dealt with extensively by researchers working in nuclear counting [38], [39] and neural counting [40], [41]. In both cases, the modified distribution is simply expressible in terms of the unmodified distribution and the deadtime ratio τ/T, where τ is the deadtime and T is the sampling time. Even small values of τ/T ($\sim$0.01) alter the distribution markedly [37] so that deadtime effects cannot in general be neglected. In a recent paper [20], we presented experimental verification of Diament and Teich's [15]-[17] theoretical photon-counting distributions for triangularly and sinusoidally modulated laser radiation and of Cantor and Teich's [37] nonparalyzable deadtime-modified versions of these formulas.

In this paper we consider likelihood-ratio detection, information transmission, and image detection in the presence of such fixed, nonparalyzable deadtime. In the counting system we consider, the source is deterministically or stochastically modulated (see Fig. 1). The input u to the detector is the binary-gated modulated signal, and its output v_1 is the number of counts registered in the fixed sampling time interval T. The output of the likelihood-ratio test v_2 is a random variable with value 1 or 0 depending on the decision. Noise arising from background and dark effects is considered to give rise to a deadtime-modified Poisson counting distribution (this may come about from a background that exhibits no intrinsic fluctuations, or from a background that is independent, noninterfering, and additive with the signal, and that has a degeneracy parameter [3] that is much less than unity). Though the Poisson condition for the background is quite generally obeyed, an arbitrary noise process can be treated within our framework at the price of increased complexity.

In Section II we consider the relevant counting distributions. Likelihood-ratio detection is treated in Section III, information transmission and channel capacity in Section IV, and image detection in Section V. The conclusions appear in Section VI.

II. Deadtime-Modified Counting Distribution for a Fluctuating Source

The nonparalyzable deadtime-modified counting distributions used in this work are obtained by the method outlined by Cantor and Teich [37], in conjunction with the results of Diament and Teich [15]-[18] for various fluctuating signal sources; Teich and Vannucci [20] have experimentally verified these expressions in the case of photon counting with sinusoidal and triangular modulation (the notation in this paper is slightly different from that used in [20], however).

In the presence of signal alone (S), the probability $p_S(n,\tau/T)$ of registering n counts in the time interval T for a detector with nonparalyzable fixed deadtime τ is [37], [20]

$$p_S(n,\tau/T)=\begin{cases}\displaystyle\sum_{k=0}^{n} p_k(n,\lambda)-\sum_{k=0}^{n-1} p_k(n-1,\lambda), & n<\dfrac{T}{\tau}\\[2ex] \displaystyle 1-\sum_{k=0}^{n-1} p_k(n-1,\lambda), & \dfrac{T}{\tau}\leqslant n<\dfrac{T}{\tau}+1.\\[2ex] 0, & n\geqslant\dfrac{T}{\tau}+1\end{cases}\tag{1}$$

Here

$$p_k(n,\lambda)=\langle\{\lambda^k[T-n\tau]^k/k!\}\exp\{-\lambda[T-n\tau]\}\rangle_\lambda,\tag{2}$$

where λ is the rate parameter driving the process. In general, when the source is a stochastically fluctuating signal, the angular brackets represent an ensemble average over the statistics of both the intrinsic source fluctuations and the imposed modulation.

When only time fluctuations are present, the overall time-integrated intensity (or energy) at the detector [3] W is

$$W=\alpha\int_t^{t+T} I(t')\,dt',\tag{3}$$

but since (1) and (2) are valid only for sampling times T short in comparison with both the intrinsic fluctuation time of the source τ_c and the period of the modulation T_M, as explicitly shown by Vannucci and Teich [42], (3) reduces to

$$W=\alpha I(t)T.\tag{4}$$

Furthermore, we choose

$$\lambda(t)=\alpha I(t),\tag{5}$$

where α is the quantum efficiency of the detector. Thus, the ensemble average represented in (2) is performed with respect to the statistics of the instantaneous energy fluctuations of the modulated source, or for fixed α, with respect to the statistics of the instantaneous fluctuations of the rate parameter λ or the intensity I. If the instantaneous rate $\lambda(t)$ is not directly proportional to the source intensity, as represented in (5), then the appropriate statistics of λ are obtained by transformation from the statistics of I. In certain applications, the statistics of λ are known directly, in which case (3)-(5) are not necessary (e.g., see [1]).

Strictly speaking, the preceding results are valid only for a counter that is unblocked at the beginning of the counting interval, though this condition may not be important in practice [20], [42], [43]. A rather different expression is obtained for the paralyzable deadtime counter [20] which we do not consider here. Expressions for the deadtime-modified mean and variance for the nonparalyzable case are available under certain conditions (they apply here though they have been derived for a related problem) [42].

The effect of modulation is to cause the mean source intensity I_S to undergo excursions between two levels I_a and I_b. The modulation depth is defined as $m=(I_b-I_a)/(I_b+I_a)$, and can take on any value between 0 and 1. As indicated previously, we assume throughout that the noise is an independent Poisson process and can therefore be represented by a constant effective intensity level I_H. The contribution of the steady noise background to the modulated signal therefore has the effect of shifting the overall mean intensity to $\bar{I}_m = \bar{I}_S + I_H$, where $\bar{I}_S$ is the mean of the modulated signal. If the modulation is symmetric, such that $\bar{I}_S = (I_a + I_b)/2$, and there are no intrinsic source fluctuations, it is not difficult to demonstrate that the effect of the noise is simply to shift the modulation depth down to an effective value $m' = m\bar{I}_S/\bar{I}_m$. In the presence of both signal (S) and noise (H), therefore, the counting distribution $p_{S+H}(n, \tau/T)$ is given by (1) and (2), using the intensity statistics appropriate for the specified modulation format. The overall mean intensity is taken as $\bar{I}_m = \bar{I}_S + I_H$, and the effective modulation depth $m' = m\bar{I}_S/\bar{I}_m$ replaces the modulation depth m used to calculated $p_S(n, \tau/T)$. The arguments are similar if the source and/or the modulation is stochastic [18], except that then $p_{S+H}(n, \tau/T)$ will not have the same form as $p_S(n, \tau/T)$ [44].

As described earlier, the noise generated by dark effects and background is assumed to be given by the deadtime-modified Poisson counting distribution $p_H(n, \tau/T)$ which, in the absence of signal, is [20], [39]-[41]

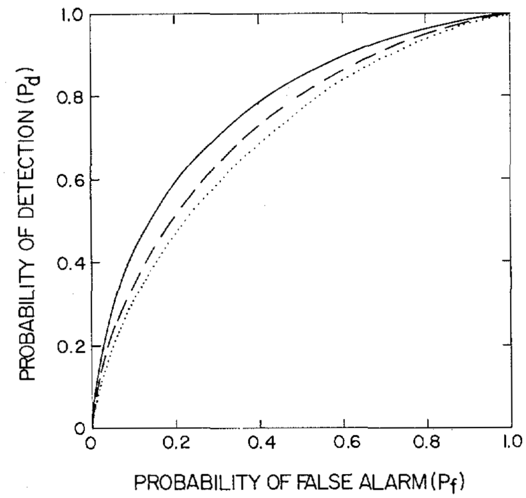

Fig. 2. Receiver operating characteristic (ROC) curves for a likelihood-ratio receiver (unmodulated amplitude-stabilized signal) in the absence of deadtime (solid curve), for the deadtime ratio $\tau/T = 0.02$ (dashed curve), and for $\tau/T = 0.05$ (dotted curve). The (fixed) unmodified signal level is $\lambda_S T = 5$, and the unmodified noise level is $\lambda_H T = 20$ for all curves.

$$p_H(n, \tau/T) = \begin{cases} \sum_{k=0}^{n} \{\lambda_H^k [T - n\tau]^k/k!\} \exp\{-\lambda_H[T - n\tau]\} - \sum_{k=0}^{n-1} \{\lambda_H^k[T - (n-1)\tau]^k/k!\} \exp\{-\lambda_H[T - (n-1)\tau]\}, & n < \dfrac{T}{\tau} \\ 1 - \sum_{k=0}^{n-1} \{\lambda_H^k [T - (n-1)\tau]^k/k!\} \exp\{-\lambda_H[T - (n-1)\tau]\}, & \dfrac{T}{\tau} \leqslant n < \dfrac{T}{\tau} + 1. \\ 0, & n \geqslant \dfrac{T}{\tau} + 1 \end{cases} \tag{6}$$

III. Likelihood-Ratio Detection in the Presence of Deadtime

Using the likelihood-ratio test for an on-off system (nonorthogonal signaling format) such as that shown in Fig. 1 [22]-[31], the decision threshold n_D is determined by the minimum count number n satisfying the condition

$$p_{S+H}(n, \tau/T)/p_H(n, \tau/T) \geqslant \Lambda, \tag{7}$$

where $p_{S+H}(n, \tau/T)$ and $p_H(n, \tau/T)$ are the counting distributions described in the previous section and Λ is the decision level. This result assumes the existence of a single decision threshold [25]. For simplicity, we assume a Bayes criterion with equal costs so that $\Lambda = (1 - Q)/Q$, where Q is the *a priori* probability that the signal is present. Maximum-likelihood detection is associated with $\Lambda = 1$ ($Q = 0.5$). In order to construct the receiver operating characteristic (ROC), we write the probability of detection P_d and the probability of false alarm P_f in terms of the parameter n_D as

$$P_d = \sum_{n=n_D}^{\infty} p_{S+H}(n, \tau/T) \tag{8}$$

and

$$P_f = \sum_{n=n_D}^{\infty} p_H(n, \tau/T). \tag{9}$$

The ROC curve is a plot of P_d versus P_f as the decision threshold n_D varies from 0 to ∞.

A. Unmodulated Amplitude-Stabilized Signal

In Fig. 2, we present ROC curves corresponding to an unmodulated ($m = 0$) amplitude-stabilized signal in the presence of a steady background (Poisson counts). The solid curve corresponds to a detector with zero deadtime, whereas the dashed curve corresponds to a ratio of deadtime to sampling time $\tau/T = 0.02$ and the dotted curve to $\tau/T = 0.05$. The unmodified (fixed) signal level $\langle n_S \rangle = \lambda_S T = 5$ and the unmodified noise level $\langle n_H \rangle = \lambda_H T = 20$ for all curves. The effect of the deadtime is to decrease the probability of detection at a fixed false-alarm rate (constant P_f). The small-signal level $\lambda_S T = 5$ was used in order to clearly illustrate this effect graphically. It is important to note that although continuous

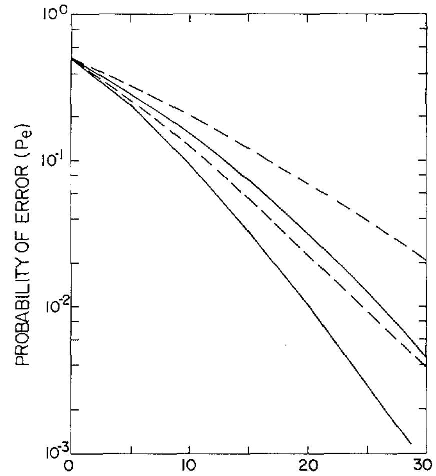

Fig. 3. Probability of error (P_e) versus signal level ($\lambda_S T$) for an unmodulated amplitude-stabilized signal in the absence of deadtime (solid curves) and with a deadtime ratio $\tau/T = 0.02$ (dashed curves). The unmodified noise level $\lambda_H T$ is 20 for the upper pair of curves and 10 for the lower pair. The *a priori* probability $Q = 0.5$ for all curves.

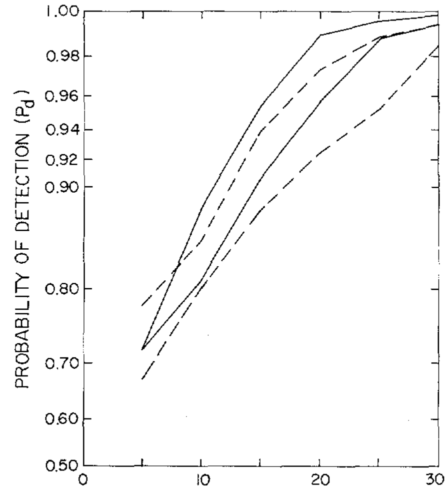

Fig. 4. Probability of detection (P_d) versus signal level ($\lambda_S T$) for an unmodulated amplitude-stabilized signal in the absence of deadtime (solid curves) and with a deadtime ratio $\tau/T = 0.02$ (dashed curves). The unmodified noise level $\lambda_H T$ is 10 for the upper pair of curves and 20 for the lower pair. The *a priori* probability $Q = 0.5$ for all curves.

curves are drawn in Fig. 2, the ROC is defined only at discrete points. This is because the decision threshold n_D takes on only integer values [26].

In terms of the parameter n_D, the total probability of error P_e is

$$P_e = Q\left[1 - \sum_{n=n_D}^{\infty} p_{S+H}(n, \tau/T)\right] + (1-Q)\sum_{n=n_D}^{\infty} p_H(n, \tau/T). \quad (10)$$

Selecting n_D in accordance with (7) for maximum-likelihood detection ($\Lambda = 1$), the total probability of error for an amplitude-stabilized source in the absence of modulation is presented in Fig. 3 as a function of the unmodified mean signal level $\lambda_S T$. The solid curves correspond to a detector with zero deadtime, whereas the dashed curves correspond to $\tau/T = 0.02$. The unmodified noise level $\lambda_H T = 10$ for the lower pair of curves and $\lambda_H T = 20$ for the upper pair. Clearly, the effect of the deadtime is to increase the probability of error in all cases.

Fig. 4 presents the probability of detection as a function of the unmodified mean signal level for a detector with zero deadtime (solid curves) and for the ratio $\tau/T = 0.02$ (dashed curves). The detection probabilities have been plotted on inverted log versus linear paper to expand the scale for high values of P_d. The unmodified noise levels are $\lambda_H T = 10$ for the upper pair of curves and $\lambda_H T = 20$ for the lower pair; the detection probabilities in Fig. 4 therefore correspond to the error probability curves in Fig. 3. Note that the probability of detection for $\lambda_H T = 10$ and $\lambda_S T < 8$ (upper pair of curves) is greater for a detector with deadtime than for one without. This higher value of P_d is accompanied, however, by an increase in the false-alarm rate P_f. This arises from the discrete nature of the processes involved; the decision threshold n_D takes on only integer values, and at threshold the ratio $p_{S+H}(n_D, \tau/T)/p_H(n_D, \tau/T)$ is not, in general, precisely equal to the decision level Λ, but is obtained from the actual point on the ROC curve.

B. *Triangularly Modulated Amplitude-Stabilized Signal*

As an example of a modulated signal, we examine the maximum-likelihood detection of a triangularly modulated amplitude-stabilized source in the presence of deadtime. For an arbitrary modulation depth m', the quantity $p_k(n, \lambda)$ expressed in (2) is [15]-[17], [37] (see also [20, eqs. (4), (7)])

$$p_k(n,\lambda) = [2m'\lambda(T - n\tau)]^{-1} \times \left\{\exp[-\lambda(T-n\tau)(1-m')]\sum_{j=0}^{k}[\lambda(T-n\tau)(1-m')]^j/j! - \exp[-\lambda(T-n\tau)(1+m')]\sum_{j=0}^{k}[\lambda(T-n\tau)(1+m')]^j/j!\right\}, \quad (11)$$

with λ and m' defined previously. It has been shown both theoretically [15]-[17] and experimentally [16], [20] that this result is very accurate for $T \ll T_M$, where T_M is the period of the modulation, and this condition is assumed throughout. The deadtime-modified distribution for the noise alone is again given by (6).

In Figs. 5 and 6 we show representative examples of the counting distributions corresponding to noise alone (dashed curves) and to signal plus noise (solid curves) for a triangularly modulated signal in the presence of a steady noise background. The unmodified noise level $\lambda_H T = 10$ and the unmodified

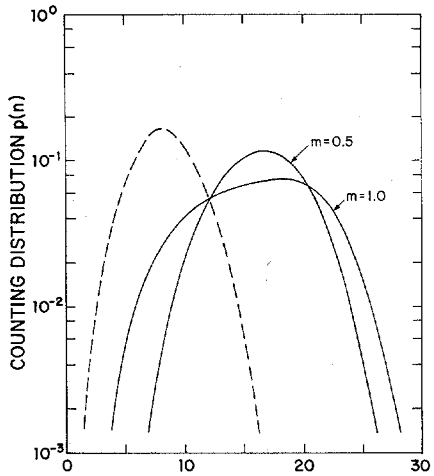

Fig. 5. Counting distributions corresponding to noise alone (dashed curve) and signal plus noise (solid curves) for a triangularly modulated amplitude-stabilized source in the presence of a steady noise background with the modulation depth m as a parameter. The unmodified noise level $\lambda_H T = 10$, the unmodified mean signal level $\lambda_S T = 15$, and the deadtime ratio $\tau/T = 0.02$ for all curves. The signal modulation depth $m = 0.5$ and 1.0 as indicated. Since the noise is unaffected by the modulation, the noise distribution (dashed curve) is the same for both cases.

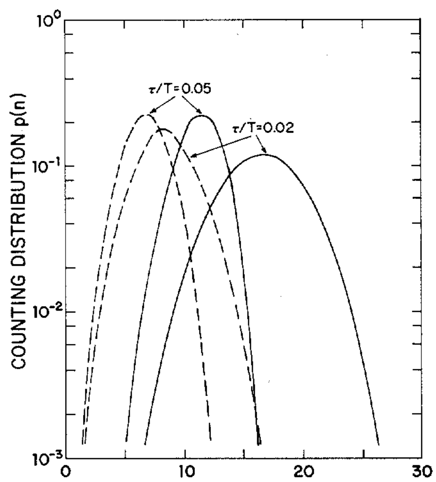

Fig. 6. Counting distributions corresponding to noise alone (dashed curves) and signal plus noise (solid curves) for a triangularly modulated amplitude-stabilized source in the presence of a steady noise background. The unmodified noise level $\lambda_H T = 10$, the unmodified mean signal level $\lambda_S T = 15$, and the signal modulation depth $m = 0.5$ for all curves. The deadtime ratio $\tau/T = 0.02$ and 0.05 as indicated.

mean signal level $\lambda_S T = 15$ for all curves. In Fig. 5 the deadtime ratio τ/T is 0.02 and the modulation depth m is 0.5 or 1.0 as indicated whereas in Fig. 6, m is constant and equal to 0.5, but τ/T takes on the two values 0.02 and 0.05 as indicated.

For maximum-likelihood detection ($Q = 0.5$), the decision threshold n_D can be determined simply by examining the intersections of the appropriate dashed and solid curves. From Fig. 5, it appears that the modulation depth m has little effect on n_D for the particular parameters used, whereas n_D changes more substantially with deadtime (see Fig. 6). This is illustrated in Fig. 7 which presents the decision threshold n_D as a function of the unmodified mean signal level $\lambda_S T$ for modula-

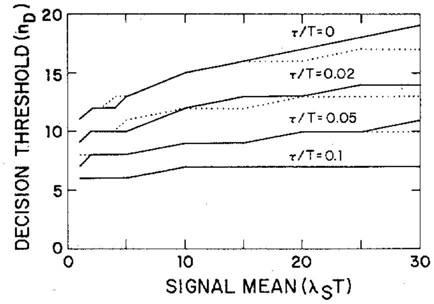

Fig. 7. Decision threshold n_D as a function of unmodified mean signal level $\lambda_S T$ for a triangularly modulated amplitude-stabilized source. The unmodified (steady) noise level $\lambda_H T = 10$ for all curves and the signal modulation depths are $m = 0.5$ (solid curves) and $m = 1.0$ (dotted curves). The deadtime ratio $\tau/T = 0$, 0.02, 0.05, and 0.1 as indicated.

tion depths $m = 0.5$ (solid curves) and $m = 1.0$ (dotted curves) with the deadtime ratio τ/T as a parameter. The steady noise level $\lambda_H T = 10$ for all cases. It is clear that the modulation has the largest effect on n_D in the absence of deadtime, and no appreciable effect on n_D in the reasonably severe deadtime-limited case ($\tau/T = 0.1$). This is not too surprising, however, since in this latter case the maximum registered count must be less than 10.

In Appendix I we present an approximate expression for the decision threshold n_D for an amplitude-stabilized signal in the absence of modulation when the mean noise count is large. This approximation was not used in any of the results presented in this paper, however, which were obtained by calculation on the Columbia University IBM OS 360/91 computer.

In Figs. 8 and 9 we present probability of error curves for a maximum-likelihood receiver detecting a triangularly modulated amplitude-stabilized signal. The solid curves represent a detector with zero deadtime, whereas the dashed curves correspond to the ratio $\tau/T = 0.02$ in all cases. The modulation depth m is 0.5 in Fig. 8 and 1.0 in Fig. 9. In both of the figures the unmodified noise level $\lambda_H T$ is 20 for the upper pair of curves and 10 for the lower pair. The effect of the triangular modulation is to broaden the counting distribution [15]-[17]; this is reflected in the higher probability of error in comparison with the unmodulated results presented in Fig. 3.

IV. Channel Capacity in the Presence of Deadtime

Whereas the probability of error, the probability of detection, and the ROC specify receiver performance, the rate of information transmission is governed by the channel capacity. We consider a communication channel in which the input U takes on the values $a_1, a_2, \cdots, a_n$, and the output V takes on the values $b_1, b_2, \cdots, b_m$. Let $r_U(a_i)$ be the probability that the input U takes on the value a_i, $i = 1, 2, \cdots, n$, and $r_V(b_j)$ the probability that the output V takes on the value b_j, $j = 1, 2, \cdots, m$. In a similar manner, we define a joint probability $r_{UV}(a_i, b_j)$ and a conditional probability $r_{V|U}(b_j | a_i)$. The mutual information $I_{U;V}(a_i; b_j)$ between the events $U = a_i$ and $V = b_j$ is given by [32], [45]-[47]

$$\begin{aligned} I_{U;V}(a_i; b_j) &= \log \{r_{UV}(a_i, b_j)/[r_U(a_i) r_V(b_j)]\} \\ &= \log \{r_{V|U}(b_j | a_i)/r_V(b_j)\}, \end{aligned} \tag{12}$$

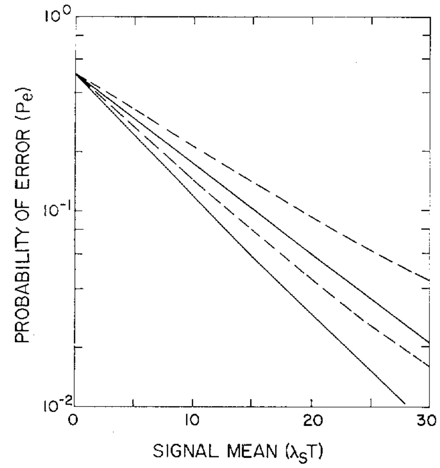

Fig. 8. Probability of error (P_e) versus unmodified mean signal level ($\lambda_S T$) for a triangularly modulated amplitude-stabilized signal in the absence of deadtime (solid curves) and with a deadtime ratio $\tau/T = 0.02$ (dashed curves). The unmodified (steady) noise level $\lambda_H T$ is 20 for the upper pair of curves and 10 for the lower pair. The signal modulation depth $m = 0.5$ and the *a priori* probability $Q = 0.5$ for all curves.

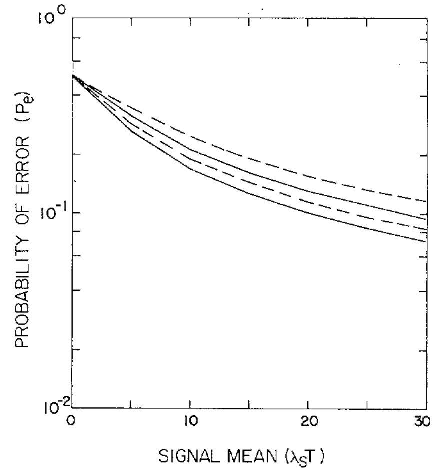

Fig. 9. Probability of error (P_e) versus unmodified mean signal level ($\lambda_S T$) for a triangularly modulated amplitude-stabilized signal in the absence of deadtime (solid curves) and with a deadtime ratio $\tau/T = 0.02$ (dashed curves). The unmodified (steady) noise level $\lambda_H T$ is 20 for the upper pair of curves and 10 for the lower pair. The signal modulation depth $m = 1.0$ and the *a priori* probability $Q = 0.5$ for all curves.

where the logarithm is usually taken to the base 2 for convenience in dealing with binary systems. The average mutual information between the input U and the output V is then

$$I(U;V) = \sum_{a_i} \sum_{b_j} r_{UV}(a_i, b_j) \log \{r_{V|U}(b_j|a_i)/r_V(b_j)\}, \quad (13)$$

which may be written for convenience as

$$I(U;V) = \sum_u \sum_v r(u,v) \log [r(v|u)/r(v)]$$
$$= \sum_u \sum_v r(v|u) r(u) \log [r(v|u)/r(v)], \quad (14)$$

where u and v represent values of the random variables U and V and $r(v|u)$ is the conditional probability. It should be noted that

$$r(v) = \sum_u r(v|u) r(u). \quad (15)$$

Now, if the conditional probability $r(v|u)$ is given for the channel, one can maximize $I(U;V)$ with respect to $r(u)$ to obtain the channel capacity C, i.e.,

$$C = \max_{r(u)} I(U;V). \quad (16)$$

In the following sections we obtain the channel capacity for the modulated-signal counting system in the presence of detector deadtime.

A. Simple Counting Receiver

Consider a binary system (see Fig. 1) in which the input U is taken to be equal to 1 when a signal is present, and 0 when the signal is absent. The output of the system V_1 is equal to the number of counts registered; thus, V_1 can take on all nonnegative integer values $0, 1, 2, \cdots, \infty$. In this subsection we exclude the likelihood-ratio test (see Fig. 1).

Letting $p(u=1) = Q$, $p(u=0) = 1 - Q$, and $p(v=n) = r(n)$, the average mutual information $I(U;V)$ given in (14) is explicitly expressible as

$$I(U;V) = \sum_{n=0}^{\infty} \Big\{ Q r(n|1) \log [r(n|1)/r(n)] + (1-Q) r(n|0) \log [r(n|0)/r(n)] \Big\}, \quad (17)$$

where we use (15) to provide

$$r(n) = Q r(n|1) + (1-Q) r(n|0). \quad (18)$$

If the likelihood-ratio test is excluded, we have $r(n|0) = p_H(n, \tau/T)$ and $r(n|1) = p_{S+H}(n, \tau/T)$ as given by (6), and by (1) and (2), respectively. With $r(n|0)$ and $r(n|1)$, we can calculate $I(U;V)$ for any given value of Q, and thus find the channel capacity C, the maximum value of $I(U;V)$ [see (16)]. For the system considered here, this quantity is a function of the source statistics, the deadtime, the modulation format and depth, and the various mean levels of signal and noise.

B. Likelihood-Ratio Counting Receiver

In this case, the output V_2 may take on only two values, 0 and 1, as determined by the likelihood-ratio test. Thus,

$$r(0|0) = \sum_{n=0}^{n_D - 1} p_H(n, \tau/T), \qquad r(1|0) = 1 - r(0|0),$$

$$r(0|1) = \sum_{n=0}^{n_D - 1} p_{S+H}(n, \tau/T), \qquad r(1|1) = 1 - r(0|1), \quad (19)$$

and the average mutual information is given by the well-known formula

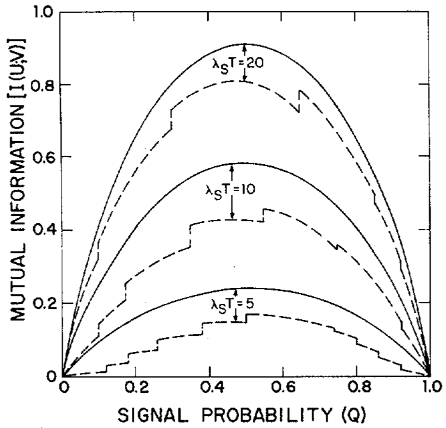

Fig. 10. Average mutual information $I(U; V)$ versus *a priori* signal probability Q for a simple counting receiver (solid curves) and for a maximum-likelihood counting receiver (dashed curves) with the unmodified signal mean $\lambda_S T$ as a parameter. The ratio of deadtime to sampling time $\tau/T = 0.02$, the unmodified noise mean $\lambda_H T = 10$, and the modulation depth $m = 0$ for all curves (amplitude-stabilized source). Unmodified signal means are $\lambda_S T = 5$, 10, and 20 as indicated. The peak of each curve represents the channel capacity.

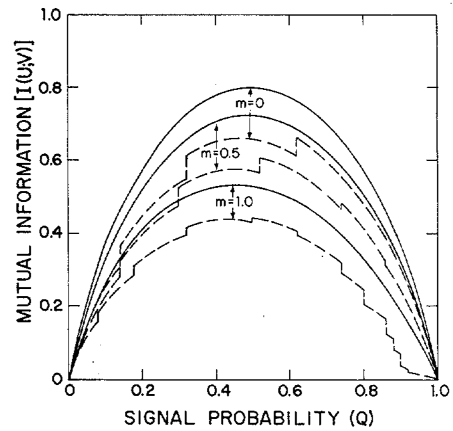

Fig. 11. Average mutual information $I(U; V)$ versus *a priori* signal probability Q for a simple counting receiver (solid curves) and for a maximum-likelihood counting receiver (dashed curves) with the (triangular) modulation depth m as a parameter. $\tau/T = 0.02$, $\lambda_S T = 15$, and $\lambda_H T = 10$ for all curves. The (signal) modulation depths are $m = 0$, 0.5, and 1.0 as indicated. The peak of each curve represents the channel capacity.

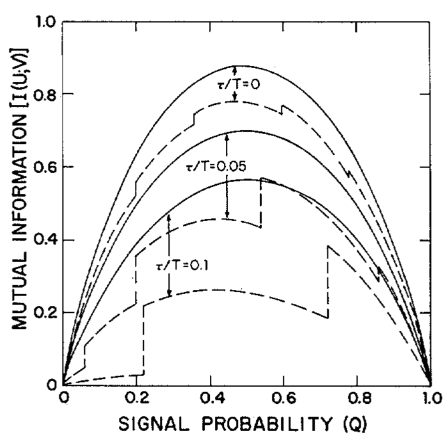

Fig. 12. Average mutual information $I(U; V)$ versus *a priori* signal probability Q for a simple counting receiver (solid curves) and for a maximum-likelihood counting receiver (dashed curves) with the deadtime ratio τ/T as a parameter. $\lambda_S T = 15$, $\lambda_H T = 10$, and $m = 0$ for all cases. Curves are shown for $\tau/T = 0$, 0.05, and 0.1 as indicated. The peak of each curve represents the channel capacity.

$$I(U; V) = \sum_{m=0}^{1} \Big\{ Q r(m \mid 1) \log [r(m \mid 1)/r(m)] + (1 - Q)\, r(m \mid 0) \log [r(m \mid 0)/r(m)] \Big\}. \tag{20}$$

In this case, $r(v \mid u)$ is a function of the *a priori* probability Q, since $r(v \mid u)$ depends on n_D, which is a function of Q.

In Figs. 10–12 we present the results for $I(U; V)$ versus Q for both types of receiver, showing the effects of a number of parameters. The solid curves refer to the simple counting receiver without the likelihood-ratio test, whereas the dashed curves represent the likelihood-ratio counting receiver. Fig. 10 shows the average mutual information for unmodified signal means $\lambda_S T = 5$, 10, and 20 for an amplitude-stabilized signal (zero modulation). The unmodified noise mean $\lambda_H T = 10$ and the ratio $\tau/T = 0.02$ for all curves. The effect of triangular modulation is displayed in Fig. 11 where $\lambda_S T = 15$, $\lambda_H T = 10$, $\tau/T = 0.02$ and the variable parameter is the modulation depth, which takes on the values $m = 0$, 0.5, and 1. Fig. 12 shows the mutual information for various values of the deadtime ratio, viz., $\tau/T = 0$, 0.05, and 0.1. The source is an amplitude-stabilized signal ($m = 0$) with unmodified signal mean $\lambda_S T = 15$, and the unmodified noise mean is $\lambda_H T = 10$. As expected, the channel capacity decreases with decreasing signal mean (Fig. 10), increasing modulation depth (Fig. 11), and increasing deadtime (Fig. 12). Note that the peak mutual information occurs at or near $Q = 0.5$ in all cases.

An obvious distinction between the two types of receiver is that the likelihood-ratio receiver exhibits discontinuities in the

$I(U; V)$ versus Q curves. This is because of the discrete nature of the decision threshold n_D which jumps from one integer to the next at certain values of Q, as Q varies. The likelihood-ratio receiver yields a lower capacity than the simple counting receiver in all cases. Since both the input and output take on the values of 0 and 1 only, with the binary counting likelihood-ratio receiver, it may be considered as an asymmetrical binary channel [47] with varying error-transition probability, i.e., $r(1|0)$ and $r(0|1)$. Thus, it is expected that the channel capacity will not exceed 1.

V. Image Detection in the Presence of Deadtime

The use of a counting array to detect a received image has been investigated by a number of authors [48]-[51]. One technique [49] is to obtain a maximum-likelihood estimate (MLE) of the mean rate at each detector in the array. In this section, we consider an elementary maximum-likelihood estimation scheme in the presence of detector deadtime. For an image illuminated by a signal that is constant in time (or by a source with degeneracy parameter [3] $\ll 1$), Poisson counting will be observed at each detector in the absence of deadtime. We assume that the statistics at each detector in the array are independent. The probability of observing n counts in a time interval T, for a single counting sample at a particular detector in the presence of a nonparalyzable deadtime τ is, from (6),

$$p(n|\lambda) = \sum_{k=0}^{n} \{\lambda^k [T - n\tau]^k/k!\} \exp\{-\lambda[T - n\tau]\} - \sum_{k=0}^{n-1} \{\lambda^k [T - (n-1)\tau]^k/k!\} \exp\{-\lambda[T-(n-1)\tau]\}, \tag{21}$$

for $n < T/\tau$. For simplicity, we do not consider the solution for the highest allowed count $(T/\tau \leqslant n < T/\tau + 1)$.

In order to obtain a maximum-likelihood estimate of the rate, denoted by λ_{MLE}, we seek the solution of

$$\partial p(n|\lambda)/\partial\lambda|_{\lambda=\lambda_{\mathrm{MLE}}} = 0. \tag{22}$$

After some algebra, it can be shown (see Appendix II) that the maximum-likelihood estimate λ_{MLE} is the solution of the transcendental equation

$$\lambda_{\mathrm{MLE}}\tau \exp(\lambda_{\mathrm{MLE}}\tau) = n\tau[T - (n-1)\tau]^n/[T - n\tau]^{n+1}, \quad n < T/\tau. \tag{23}$$

Equation (23) can be solved by an application of Newton's method [52] to yield a value for λ_{MLE} to any desired accuracy. In the limit, as $\tau/T \to 0$, (23) reduces to the zero-deadtime result obtained for a single sampling [49], i.e.,

$$\lambda_{\mathrm{MLE}} = n/T. \tag{24}$$

An approximate closed form solution for λ_{MLE} can be obtained in the two limiting cases $\lambda_{\mathrm{MLE}}\tau \ll 1$ and $\lambda_{\mathrm{MLE}}\tau \gg \ln \lambda_{\mathrm{MLE}}\tau$. For $\lambda_{\mathrm{MLE}}\tau \ll 1$, $\exp(\lambda_{\mathrm{MLE}}\tau) \simeq 1 + \lambda_{\mathrm{MLE}}\tau$, and λ_{MLE} can be obtained as the solution to the quadratic equation

$$\lambda_{\mathrm{MLE}}\tau(1 + \lambda_{\mathrm{MLE}}\tau) = n\tau[T-(n-1)\tau]^n/[T-n\tau]^{n+1}. \tag{25}$$

For the opposite limiting case, we take the natural logarithm of (23), yielding

$$\ln \lambda_{\mathrm{MLE}}\tau + \lambda_{\mathrm{MLE}}\tau = \ln\{n\tau[T-(n-1)\tau]^n/[T-n\tau]^{n+1}\}; \tag{26}$$

for $\lambda_{\mathrm{MLE}}\tau \gg \ln \lambda_{\mathrm{MLE}}\tau$ (which is valid for $\lambda_{\mathrm{MLE}}\tau \gtrsim 30$), the solution is

$$\lambda_{\mathrm{MLE}} \simeq \tau^{-1} \ln\{n\tau[T-(n-1)\tau]^n/[T-n\tau]^{n+1}\}. \tag{27}$$

The statistical confidence level γ [49], [53] of the maximum-likelihood estimate can be computed under the assumption of Bayesian statistics as

$$\gamma = \int_{\lambda_{\mathrm{MLE}}-\alpha}^{\lambda_{\mathrm{MLE}}+\beta} p(\lambda|n)\, d\lambda. \tag{28}$$

The range of values in λ, $\lambda_{\mathrm{MLE}} - \alpha$ to $\lambda_{\mathrm{MLE}} + \beta$, required to reach a prescribed value of γ is the confidence interval. With the use of the axioms of Bayesian statistics, (28) may be written as

$$\gamma = \int_{\lambda_{\mathrm{MLE}}-\alpha}^{\lambda_{\mathrm{MLE}}+\beta} p(n|\lambda)p(\lambda)\, d\lambda \Bigg/ \int_0^\infty p(n|\lambda)p(\lambda)\, d\lambda, \tag{29}$$

where $p(\lambda)$ is the probability density of the mean rate of the counting distributions. In the limit, as $p(\lambda)$ becomes a very wide distribution, the confidence level as given by (28) becomes

$$\gamma = \int_{\lambda_{\mathrm{MLE}}-\alpha}^{\lambda_{\mathrm{MLE}}+\beta} p(n|\lambda)\, d\lambda. \tag{30}$$

Since the expression in (30) involves integrals over terms which are Poisson in nature [see (21)], classical statistical tables may be used to obtain the confidence interval, once a value of γ is chosen.

To increase the accuracy of the estimate, the count could be sampled N times, rather than once, at each detector. There would then be N values of the observed count number: $n_1, n_2, \cdots, n_N$. The maximum-likelihood estimate of λ would then be obtained by maximizing the N-fold joint probability of observing n_1 counts in time interval 1, n_2 counts in time interval 2, and so on, up to the Nth time interval. For Poisson counting in the presence of a fixed deadtime, if the intervals can be assumed to be independent, the joint probability distribution simply reduces to the product of the individual distributions

$$p(n_1, n_2, \cdots, n_N|\lambda) = \prod_{i=1}^{N} p(n_i|\lambda), \tag{31}$$

with the $p(n_i|\lambda)$ given by (21). (The higher order (joint) statistics frequently provide useful information about a system in the nonindependent case.) The maximum-likelihood estimate of the rate parameter, λ_{MLE}, is obtained from

$$\partial p(n_1, n_2, \cdots, n_N|\lambda)/\partial\lambda|_{\lambda=\lambda_{\mathrm{MLE}}} = 0. \tag{32}$$

The solution to this equation, using the joint density function given in (31), entails a great deal of algebra inasmuch as each of the $p(n_i|\lambda)$ consists of a summation of many terms. Thus, the joint density involves a large number of product terms, and (32) would have to be solved by numerous applications of the chain rule for differentiation. The solution could be greatly simplified, however, by using the approximate form for $p(n_i/\lambda)$ given in [20] and in Appendix II.

VI. Conclusion

Expressions have been obtained for the fixed-time-interval counting distributions for a periodically or stochastically varying signal in the presence of Poisson noise counts and fixed nonparalyzable deadtime. For symmetric modulation, in the absence of intrinsic source fluctuations, it has been shown that additive amplitude-stabilized noise affects the total signal by shifting the mean intensity upward, thereby introducing an effective modulation depth.

Likelihood-ratio receiver performance and information rate were evaluated for a number of specific cases. ROC curves were presented for an unmodulated amplitude-stabilized signal illustrating that the deadtime causes an increase in the false-alarm probability for a fixed probability of detection, or equivalently, a lower probability of detection for a fixed false-alarm rate.

Representative deadtime-modified counting distributions were presented for noise alone and for signal plus noise with various values of deadtime and (triangular) modulation depth. The behavior of the decision threshold was examined graphically, and it was demonstrated that the presence of modulation has relatively little effect on the decision threshold, especially when the system is highly deadtime-limited. An approximate analytic expression for n_D, valid for an unmodulated amplitude-stabilized signal and small deadtime, shows that the effect of the deadtime is to reduce the decision threshold.

Probability of error and probability of detection curves were provided for an unmodulated and for a triangularly modulated amplitude-stabilized source. The effect of both the deadtime and the modulation was to increase the probability of error. In the case of modulation this occurred as a result of a broadening of the constituent probability distributions, whereas in the case of deadtime, it arose from a loss of counts.

The average mutual information was presented as a function of the *a priori* signal probability Q for unmodulated and for triangularly modulated amplitude-stabilized sources. The channel capacity was shown to decrease with increasing deadtime, increasing modulation depth, and decreasing signal mean; it was always greater for the simple counting receiver than for the likelihood-ratio counting receiver.

Finally, a maximum-likelihood estimate of the mean signal level for a simple image detection system with a deadtime-perturbed counting array was presented; approximate closed-form solutions were obtained in certain limiting cases. An expression for the statistical confidence level of the estimate was obtained, and a technique was proposed for possibly increasing this confidence level by multiple sampling.

Inasmuch as the results obtained here apply to an arbitrary deadtime-perturbed doubly stochastic Poisson counting system, they are expected to find application in such diverse areas as optical photocounting communications, operations research, nuclear counting, and neural counting and psychophysics, where there exists substantial evidence of the importance of deadtime effects. Thus, for example, a special case of our results provides the channel capacity and error rate for the receptive-field-to-ganglion-cell visual pathway in the cat's retina for various conditions under which the maintained discharge is observed [41].

Clearly, calculations of the kind performed here can be extended in the direction of orthogonal signal sets [54], joint-counting statistics [19], joint likelihood detection, suboptimum receiver structures, and M-ary signaling. The detection law [4], [55] appropriate to any particular set of conditions could also be investigated.

Appendix I
Decision Threshold for Large Mean Noise Count

The decision threshold n_D in the presence of detector deadtime for an amplitude-stabilized signal in the absence of modulation is obtained by solving the equation

$$p_{S+H}(n_D, \tau/T)/p_H(n_D, \tau/T) = \Lambda. \tag{A1}$$

We consider maximum-likelihood detection so that $\Lambda = 1$. It is in general difficult to obtain an analytical solution to (A1); nevertheless, an approximate expression for n_D can be obtained when the mean noise count (and therefore the mean signal plus noise count) is large. In that case, the deadtime-modified counting distributions can be approximated as [20]

$$p_{S+H}(n_D, \tau/T) = \{[\lambda_S + \lambda_H]^{n_D} [T - n_D\tau]^{n_D}/n_D!\} \cdot \exp\{-[\lambda_S + \lambda_H][T - n_D\tau]\} \tag{A2}$$

and

$$p_H(n_D, \tau/T) = \{\lambda_H^{n_D} [T - n_D\tau]^{n_D}/n_D!\} \cdot \exp\{-\lambda_H[T - n_D\tau]\}. \tag{A3}$$

Substitution of (A2) and (A3) into (A1) yields

$$[\lambda_S + \lambda_H]^{n_D} \exp\{-\lambda_S[T - n_D\tau]\} \simeq \lambda_H^{n_D}. \tag{A4}$$

Multiplying (A4) by T^{n_D} and taking the logarithm provides

$$n_D \ln\{(\lambda_S + \lambda_H)T\} - \lambda_S\{T - n_D\tau\} \simeq n_D \ln(\lambda_H T), \tag{A5}$$

which gives rise to the desired result

$$n_D \simeq \lambda_S T\,[\ln(1 + \lambda_S/\lambda_H) + \lambda_S\tau]^{-1}. \tag{A6}$$

In the limit, as $\tau \to 0$, this properly reduces to the zero-deadtime result [23], [26], [27]

$$n_D = \lambda_S T\,[\ln(1 + \lambda_S/\lambda_H)]^{-1}. \tag{A7}$$

Appendix II
Solution for the Maximum-Likelihood Estimate of the Rate (λ_{MLE})

To obtain the maximum-likelihood estimate of the rate λ_{MLE} in the presence of deadtime, we seek the solution of

$$\partial p(n|\lambda)/\partial\lambda|_{\lambda=\lambda_{MLE}} = 0, \tag{B1}$$

with $p(n|\lambda)$ given by (21). We first compute derivatives of the form

$$(\partial/\partial\lambda)(\{\lambda^k[T-n\tau]^k/k!\}\exp\{-\lambda[T-n\tau]\})$$
$$= \{k\lambda^{k-1}[T-n\tau]^k/k!\}\exp\{-\lambda[T-n\tau]\} - [T-n\tau]\{\lambda^k[T-n\tau]^k/k!\}\exp\{-\lambda[T-n\tau]\}, \quad k \geqslant 1. \quad \text{(B2)}$$

For $k = 0$, the derivative is

$$(\partial/\partial\lambda)(\exp\{-\lambda[T-n\tau]\}) = -[T-n\tau]\exp\{-\lambda[T-n\tau]\}, \quad \text{(B3)}$$

and the overall derivative in (B1) becomes

$$\begin{aligned}\partial p(n|\lambda)/\partial\lambda = &-[T-n\tau]\exp\{-\lambda[T-n\tau]\} \\ &+\sum_{k=1}^{n}\{k\lambda^{k-1}[T-n\tau]^k/k!\}\exp\{-\lambda[T-n\tau]\} \\ &-\sum_{k=1}^{n}[T-n\tau]\{\lambda^k[T-n\tau]^k/k!\}\exp\{-\lambda[T-n\tau]\} + [T-(n-1)\tau]\exp\{-\lambda[T-(n-1)\tau]\} \\ &-\sum_{k=1}^{n-1}\{k\lambda^{k-1}[T-(n-1)\tau]^k/k!\}\exp\{-\lambda[T-(n-1)\tau]\} \\ &+\sum_{k=1}^{n-1}[T-(n-1)\tau]\{\lambda^k[T-(n-1)\tau]^k/k!\}\exp\{-\lambda[T-(n-1)\tau]\}, \qquad n < T/\tau. \quad \text{(B4)}\end{aligned}$$

Letting $j = k + 1$ in the second and fourth summations yields

$$\begin{aligned}\partial p(n|\lambda)/\partial\lambda = &-[T-n\tau]\exp\{-\lambda[T-n\tau]\} \\ &+\sum_{k=1}^{n}\{\lambda^{k-1}[T-n\tau]^k/(k-1)!\}\exp\{-\lambda[T-n\tau]\} \\ &-\sum_{j=2}^{n+1}\{\lambda^{j-1}[T-n\tau]^j/(j-1)!\}\exp\{-\lambda[T-n\tau]\} + [T-(n-1)\tau]\exp\{-\lambda[T-(n-1)\tau]\} \\ &-\sum_{k=1}^{n-1}\{\lambda^{k-1}[T-(n-1)\tau]^k/(k-1)!\}\exp\{-\lambda[T-(n-1)\tau]\} \\ &+\sum_{j=2}^{n}\{\lambda^{j-1}[T-(n-1)\tau]^j/(j-1)!\}\exp\{-\lambda[T-(n-1)\tau]\}, \quad \text{(B5)}\end{aligned}$$

which reduces to two terms, so that

$$\begin{aligned}\partial p(n|\lambda)/\partial\lambda = &-\{\lambda^n[T-n\tau]^{n+1}/n!\}\exp\{-\lambda[T-n\tau]\} \\ &+\{\lambda^{n-1}[T-(n-1)\tau]^n/(n-1)!\} \\ &\exp\{-\lambda[T-(n-1)\tau]\}. \quad \text{(B6)}\end{aligned}$$

The estimate λ_{MLE} is obtained by setting the derivative in (B6) equal to 0, i.e.,

$$\{\lambda_{\mathrm{MLE}}^n[T-n\tau]^{n+1}/n!\}\exp\{-\lambda_{\mathrm{MLE}}[T-n\tau]\} = \{\lambda_{\mathrm{MLE}}^{n-1}[T-(n-1)\tau]^n/(n-1)!\}\exp\{-\lambda_{\mathrm{MLE}}[T-(n-1)\tau]\} \quad \text{(B7)}$$

which reduces to the final result

$$\lambda_{\mathrm{MLE}}\tau\exp(\lambda_{\mathrm{MLE}}\tau) = n\tau[T-(n-1)\tau]^n/[T-n\tau]^{n+1}, \quad n < T/\tau. \quad \text{(B8)}$$

References

[1] M. Greenwood and G. U. Yule, "An inquiry into the nature of frequency distributions representative of multiple happenings with particular reference to the occurrence of multiple attacks of disease or of repeated accidents," *J. Royal Stat. Soc.*, ser. A, vol. 83, pp. 255–279, 1920.

[2] E. M. Purcell, "Correlation in the fluctuations of two photoelectric currents evoked by coherent beams of light," *Nature*, vol. 178, pp. 1449–1450, 1956.

[3] L. Mandel, "Fluctuations of photon beams and their correlations," *Proc. Phys. Soc.*, vol. 72, pp. 1037–1048, 1958; "Fluctuations of photon beams: The distribution of the photoelectrons," *Proc. Phys. Soc.*, vol. 74, pp. 233–243, 1959.

[4] W. J. McGill, "Neural counting mechanisms and energy detection in audition," *J. Math. Psychol.*, vol. 4, pp. 351–376, 1967.

[5] M. C. Teich and W. J. McGill, "Neural counting and photon counting in the presence of dead time," *Phys. Rev. Lett.*, vol. 36, pp. 754–758, 1473, 1976.

[6] J. Peřina, "Superposition of coherent and incoherent fields," *Phys. Lett.*, vol. 24A, pp. 333–334, 1967; "Superposition of thermal and coherent fields," in *Acta Universitatis Palackianae Olomucensis Facultas Rerum Naturalium*, Olomouc, Czechoslovakia, 1968, vol. 27, pp. 227–234.

[7] —, *Coherence of Light*. London: Van Nostrand-Reinhold, 1972.

[8] E. Parzen, *Stochastic Processes*. San Francisco: Holden-Day, 1962, pp. 117–186.

[9] C. Palm, "Intensitätsschwankungen im Fernsprechverkehr," *Ericsson Technics*, Stockholm, vol. 44, pp. 1–189, 1943.

[10] D. R. Cox and W. L. Smith, "The superposition of several strictly periodic sequences of events," *Biometrika*, vol. 40, pp. 1–11, 1953; "On the superposition of renewal processes," *Biometrika*, vol. 41, pp. 91–99, 1954.

[11] E. Cinlar, "Superposition of point processes," in *Stochastic Point Processes: Statistical Analysis, Theory, and Applications*, P. A. W. Lewis, Ed. New York: Wiley-Interscience, 1972, pp. 549–606, and references contained therein.

[12] R. J. Glauber, "The quantum theory of optical coherence," *Phys.*

Rev., vol. 130, pp. 2529–2539, 1963; "Coherent and incoherent states of the radiation field," *Phys. Rev.*, vol. 131, pp. 2766–2788, 1963.

[13] P. L. Kelley and W. H. Kleiner, "Theory of electromagnetic field measurement and photoelectron counting," *Phys. Rev.*, vol. 136, pp. A316–A334, 1964.

[14] D. Stoler, "Photon antibunching and possible ways to observe it," *Phys. Rev. Lett.*, vol. 33, pp. 1397–1400, 1974.

[15] M. C. Teich and P. Diament, "Flat counting distribution for triangularly-modulated Poisson process," *Phys. Lett.*, vol. 30A, pp. 93–94, 1969.

[16] ——, "Observation of flat counting distribution for Poisson process with linearly-swept mean," *J. Appl. Phys.*, vol. 41, pp. 415–416, 1970.

[17] P. Diament and M. C. Teich, "Photoelectron-counting distributions for irradiance-modulated radiation," *J. Opt. Soc. Am.*, vol. 60, pp. 682–689, 1970.

[18] ——, "Photodetection of low-level radiation through the turbulent atmosphere," *J. Opt. Soc. Am.*, vol. 60, pp. 1489–1494, 1970.

[19] M. C. Teich and S. Rosenberg, "*N*-fold joint photocounting distribution for modulated laser radiation: Transmission through the turbulent atmosphere," *J. Opto-Electron.*, vol. 3, pp. 63–76, 1971.

[20] M. C. Teich and G. Vannucci, "Observation of dead-time-modified photon-counting distributions for modulated laser radiation," *J. Opt. Soc. Am.*, vol. 68, pp. 1338–1342, 1978.

[21] D. L. Snyder, *Random Point Processes*. New York: Wiley, 1975.

[22] B. Reiffen and H. Sherman, "An optimum demodulator for Poisson processes: Photon source detectors," *Proc. IEEE*, vol. 51, pp. 1316–1320, 1963.

[23] G. W. Flint, "Analysis and optimization of laser ranging techniques," *IEEE Trans. on Military Electron.*, vol. MIL-8, pp. 22–28, 1964.

[24] C. W. Helstrom, "The detection and resolution of optical signals," *IEEE Trans. Inform. Theory*, vol. IT-10, pp. 275–287, 1964.

[25] M. C. Teich, P. R. Prucnal, and G. Vannucci, "Optimum photon detection with a simple counting processor," *Opt. Lett.*, vol. 1, pp. 208–210, 1977.

[26] H. L. Van Trees, *Detection, Estimation, and Modulation Theory*, part 1. New York: Wiley, 1968.

[27] W. K. Pratt, *Laser Communication Systems*. New York: Wiley, 1969.

[28] M. Gagliardi and S. Karp, *Optical Communications*. New York: Wiley, 1976.

[29] C. W. Helstrom, *Quantum Detection and Estimation Theory*. New York: Academic, 1976.

[30] D. M. Green and J. A. Swets, *Signal Detection Theory and Psychophysics*. New York: Wiley, 1966 [reprinted by Robert E. Krieger Publishing Co., Huntington, NY, 1974].

[31] J. P. Egan, *Signal Detection Theory and ROC Analysis*. New York: Academic, 1975.

[32] C. E. Shannon, "A mathematical theory of communication," *Bell Syst. Tech. J.*, vol. 27, pp. 379–423, 623–656, 1948.

[33] T. E. Stern, "Some quantum effects in information channels," *IRE Trans. Inform. Theory*, vol. IT-6, pp. 435–440, 1960; "Information rates in photon channels and photon amplifiers," in *IRE Int. Conv. Rec.*, part 4, 1960, pp. 182–188.

[34] J. P. Gordon, "Quantum effects in communication systems," *Proc. IRE*, vol. 50, pp. 1898–1908, 1962.

[35] B. E. Goodwin and L. P. Bolgiano, Jr., "Information capacity of a photoelectric detector," *Proc. IEEE*, vol. 53, pp. 1745–1746, 1965; G. L. Fillmore and G. Lachs, "Information rates for photocount detection systems," *IEEE Trans. Inform. Theory*, vol. IT-15, pp. 465–468, 1969.

[36] F. T. S. Yu, *Optics and Information Theory*. New York: Wiley, 1976.

[37] B. I. Cantor and M. C. Teich, "Dead-time-corrected photocounting distributions for laser radiation," *J. Opt. Soc. Am.*, vol. 65, pp. 786–791, 1975.

[38] I. DeLotto, P. F. Manfredi, and P. Principi, "Counting statistics and dead-time losses, part 1," *Energia Nucleare*, vol. 11, pp. 557–564, 1964.

[39] J. W. Müller, "Dead-time problems," *Nucl. Instr. Meth.*, vol. 112, pp. 47–57, 1973; "Some formulae for a dead-time-distorted Poisson process," *Nucl. Instr. Meth.*, vol. 117, pp. 401–404, 1974.

[40] L. M. Ricciardi and F. Esposito, "On some distribution functions for non-linear switching elements with finite dead time," *Kybernetik*, vol. 3, pp. 148–152, 1966.

[41] M. C. Teich, L. Matin, and B. I. Cantor, "Refractoriness in the maintained discharge of the cat's retinal ganglion cell," *J. Opt. Soc. Am.*, vol. 68, pp. 386–402, 1978.

[42] G. Vannucci and M. C. Teich, "Effects of rate variation on the counting statistics of dead-time-modified Poisson processes," *Opt. Commun.*, vol. 25, pp. 267–272, 1978.

[43] J. Libert, "Comparaison des distributions statistiques de comptage des systèmes radioactifs," *Nucl. Instr. Meth.*, vol. 136, pp. 563–568, 1976.

[44] M. C. Teich and R. Y. Yen, "Photocounting receiver performance for detection of multimode laser or scattered radiation," *IEEE Trans. Aerosp. Electron. Syst.*, vol. AES-8, pp. 13–18, 1972.

[45] R. G. Gallagher, *Information Theory and Reliable Communication*. New York: Wiley, 1968, p. 18.

[46] R. B. Ash, *Information Theory*. New York: Wiley-Interscience, 1965, pp. 1–26, 46–50.

[47] C. W. McMullen, *Communication Theory Principles*. New York: Macmillan, 1968, p. 268.

[48] C. W. Helstrom, "Detection and resolution of incoherent objects by a background-limited optical system," *J. Opt. Soc. Am.*, vol. 59, pp. 164–175, 1969.

[49] J. Amoss and F. Davidson, "Detection of weak optical images with photon counting techniques," *Appl. Opt.*, vol. 11, pp. 1793–1800, 1972.

[50] F. Davidson and J. Amoss, "Sequential photon-counting statistics and maximum-likelihood estimation techniques for gaussian optical fields," *J. Opt. Soc. Am.*, vol. 63, pp. 30–37, 1973.

[51] F. Davidson and R. S. Iyer, "Estimation of optical field mean intensities from photocount correlations," *Appl. Opt.*, vol. 13, pp. 2171–2176, 1974.

[52] G. B. Thomas, Jr., *Calculus and Analytic Geometry*. Reading, MA: Addison-Wesley, 1966, pp. 451–454.

[53] M. Tribus, *Rational Descriptions, Decisions, and Designs*. New York: Pergamon, 1969, pp. 442–448.

[54] L. Stephens and F. Davidson, "Photoelectron counter dead time effects on direct detection optical communication systems," *IEEE Trans. Commun.*, vol. COM-25, pp. 615–621. 1977.

[55] E. Hoversten, "Optical communication theory," in *Laser Handbook*, vol. 2, F. T. Arecchi and E. O. Schulz-DuBois, Eds. Amsterdam: North-Holland, 1972, pp. 1839–1840.